

Novel Polyhedral Oligomeric Silsesquioxane-Substituted Dendritic Polyester Tougheners for Linear Thermoplastic Polyurethane

Steven Spoljaric, Robert A. Shanks

CRC for Polymers, RMIT University, Melbourne, Victoria 3001, Australia

Received 6 October 2011; accepted 8 January 2012

DOI 10.1002/app.36773

Published online in Wiley Online Library (wileyonlinelibrary.com).

ABSTRACT: Boltorn hyperbranched aliphatic polyesters were functionalized with polyhedral oligomeric silsesquioxane (POSS) and incorporated into linear thermoplastic polyurethane (TPU). Increasing POSS-functionalized Boltorn concentration led to an increase in agglomerate size and frequency, due to interactions between POSS molecules. The Boltorn dendrimer primarily influenced the morphology of the blends. Blends displayed enhanced thermal stability, due to restrictions on chain segmental motions imparted by the Boltorn and thermal shielding by POSS. Increasing the blend concentration resulted in higher tensile modulus and strength, while ductility decreased due to increased rigidity. Creep deformation

decreased and permanent deformation increased with increased Boltorn content, while E' , E'' , and T_g values all increased. TPU blended with higher generation functionalized-Boltorn displayed superior thermal and mechanical properties than those containing lower generation dendrimer, due to enhanced interaction and restrictions on TPU chain segments. Both the Boltorn and POSS contributed to material properties. © 2012 Wiley Periodicals, Inc. *J Appl Polym Sci* 000: 000–000, 2012

Key words: dendrimers; POSS; functionalization of polymers; polyurethanes; mechanical properties; elastomers

INTRODUCTION

In an important class of dendritic polymers, *hyperbranched* polymers have attracted significant attention due to their unique three-dimensional architecture, simple synthesis, and useful properties such as high reactivity, high solubility, and low viscosity. Aliphatic hyperbranched polyesters based on dimethylolpropionic acid have been extensively studied since their introduction in 1993¹ and commercialization by Pertorp under the trade name Boltorn.² The chemical structure of the Boltorn family of dendrimers contains hydroxyl end groups, allowing for the introduction of functional groups. This versatility has led to these hyperbranched polymers finding use in various fields, including coating, drug delivery, and processing aid applications.² Boltorn dendrimers have been blended with other polymers,³ most often used as crosslinking agents in polyurethane^{4–6} and tougheners in epoxy resins.^{7–10} Although various inorganic groups have been introduced onto the Boltorn structure, including silicate¹¹

and montmorillonite clay,¹² no research has been performed regarding the incorporation of inorganic functionalized Boltorn into polymers and the influence these hybrid organic–inorganic materials have on thermal stability and thermomechanical properties.

Polyhedral oligomeric silsesquioxanes (POSS, empirical formula $\text{RSiO}_{1.5}$) are a hybrid organic–inorganic class of molecule, consisting of a rigid inorganic core made up of silicon atoms linked by oxygen atoms, with organic “R” substituents attached at the corners of the silica cage. Their name is derived from the noninteger (one and one-half or *sesqui*) ratio between the silicon and oxygen atoms and the organic substituents.¹³ The central core is ceramic in nature, providing thermal stability and rigidity, while the organic groups compatibilize the molecule, allowing it to dissolve in polymers, solvents, or coatings.¹⁴

First synthesized in 1946 by Scott,¹⁵ POSS has begun to attract attention as fillers in polymer nanocomposites within the last 10–15 years. In addition, their intrinsic properties and broad range of architectures/conformations make POSS a suitable candidate for use as functional groups, providing mechanical and thermal reinforcement. By functionalizing dendrimers with POSS and incorporating them into a linear polymer matrix, mechanical strength and thermal stability can be significantly

Correspondence to: S. Spoljaric (s.spoljaric@student.rmit.edu.au).

Contract grant sponsor: CRC for Polymers.

enhanced. POSS provides the polymer with rigidity and strength, while shielding segments of polymer chain from thermal degradation. The dendrimers entangle throughout the polymer matrix, restricting chain motions that in turn influence material properties. Furthermore, the hyperbranched macromolecules compatibilize the POSS with the linear polymer matrix, allowing applied stress to transfer from the latter to the former.

The aim was to prepare POSS-functionalized Boltorn-thermoplastic polyurethane (TPU) blends, where the treated dendritic polymers will enhance thermal stability and thermomechanical properties. Both TPU and Boltorn polymers possessed a polyester chemical structure, allowing for a high degree of compatibility. Objectives included functionalizing Boltorn dendrimers with POSS, blending the treated hyperbranched polymers with TPU, and evaluating the thermal stability and thermomechanical properties of the blends.

EXPERIMENTAL

Materials

Pellethane 2101-85A thermoplastic (polyester) polyurethane (density 1.14 g cm^3) was obtained from Dow Plastics. Boltorn dendritic polymers were obtained from Perstorp Specialty Chemicals AB, Sweden. Boltorn H20 and H40 are hyperbranched aliphatic polyesters with molecular weights of 2100 and 5100 g mol^{-1} ,¹⁶ respectively. Boltorn H20 contains 16 hydroxyl groups while Boltorn H40 contains 64. Trisilanolheptisobutyl POSS (SO1450) was obtained from Hybrid Plastics, Hattiesburg, USA.

Preparation of POSS-functionalized Boltorn

Preparation of amino-treated POSS

Trisilanolheptisobutyl POSS (5.00 g, 6.32 mmol) and 3-aminopropyltriethoxysilane (1.44 g, 6.5 mmol) were dispersed in 40 mL tetrahydrofuran (THF) and stirred at room temperature overnight. The solution was poured into 100 mL methanol and stirred for 10 min, before being suction filtered, washed with methanol, and deionized water and dried in a vacuum oven at 75°C for 12 h.

Reaction of Boltorn with treated POSS

Boltorn H20 or H40 (1 mmol) was dispersed in 150 mL of THF and stirred at room temperature for 2 h. Amino-treated isobutyl POSS (1 mmol) was added, and the solution was stirred for a further 24 h at room temperature. The solution was cast into glass Petri dishes, and the solvent was allowed to evaporate in air overnight. The POSS-functionalized dendritic polymer was washed with acetone and methanol and dried in a vacuum oven at 25°C for 12 h.

The POSS-functionalized Boltorn (Fig. 1) was stored in sealed plastic bags kept in a desiccator at 0% relative humidity. FTIR absorbance spectra were used to determine the number of POSS molecules bonded to a single Boltorn dendrimer. The method of calculation is detailed in Appendix. Eight POSS molecules were bonded to one Boltorn H20 dendrimer, while 31 POSS molecules were bonded to one Boltorn H40 dendrimer.

Preparation of PU-Boltorn-POSS blends

TPU was dissolved in a minimal amount of THF at room temperature. POSS-functionalized Boltorn was added to the solution and subjected to ultrasonic disruption (10 min, 25°C , 20 kHz) to ensure even distribution. The solution was poured into an excess of methanol to precipitate the blend and to restrict filler migration. The sample was isolated using suction filtration and dried in a vacuum oven at 35°C for 12 h.

Characterization of nanocomposites

Structural analysis

A Perkin-Elmer Spectrum 2000 FTIR spectrometer working in diffuse reflectance spectroscopy (DRIFTS) mode was used to characterize the molecular vibration of the functional groups in the POSS and Boltorn dendrimers. Anhydrous potassium bromide (KBr) was used as dispersing material, and all spectra were scanned within the range $400\text{--}4000 \text{ cm}^{-1}$, with a total of 20 scans, and a resolution of 8 cm^{-1} .

Morphological analysis

Scanning electron microscopy images of the nanocomposites were taken using a FEI Quanta 200 environmental scanning electron microscope operating at 20 kV. Composites with average dimensions $\sim 4.00 \times 4.00 \times 0.70 \text{ mm}^3$ were mounted to the specimen holder using carbon tape.

Small angle X-ray scattering

A Bruker AXS Nanostar was used to study the morphology of the polymer composites. A Cu X-ray source ($\lambda = 0.1542 \text{ nm}$) was generated at $\text{kV} = 40$ and $\text{mV} = 35$. The distance from the sample to detector was 106 cm. The radius of gyration (R_g) of polymer materials was determined by plotting $\ln(I)$ versus q^2 . This gives a linear graph from which the slope can be substituted into eq. (1) to obtain R_g .

$$-\text{slope} = \frac{R_g^2}{3} \quad (1)$$

Porod plots were constructed [$\log(I)$ vs. $\log(q)$], using the slope to determine the fractal dimension (D_f) of the blends as shown in eqs. (2) and (3).

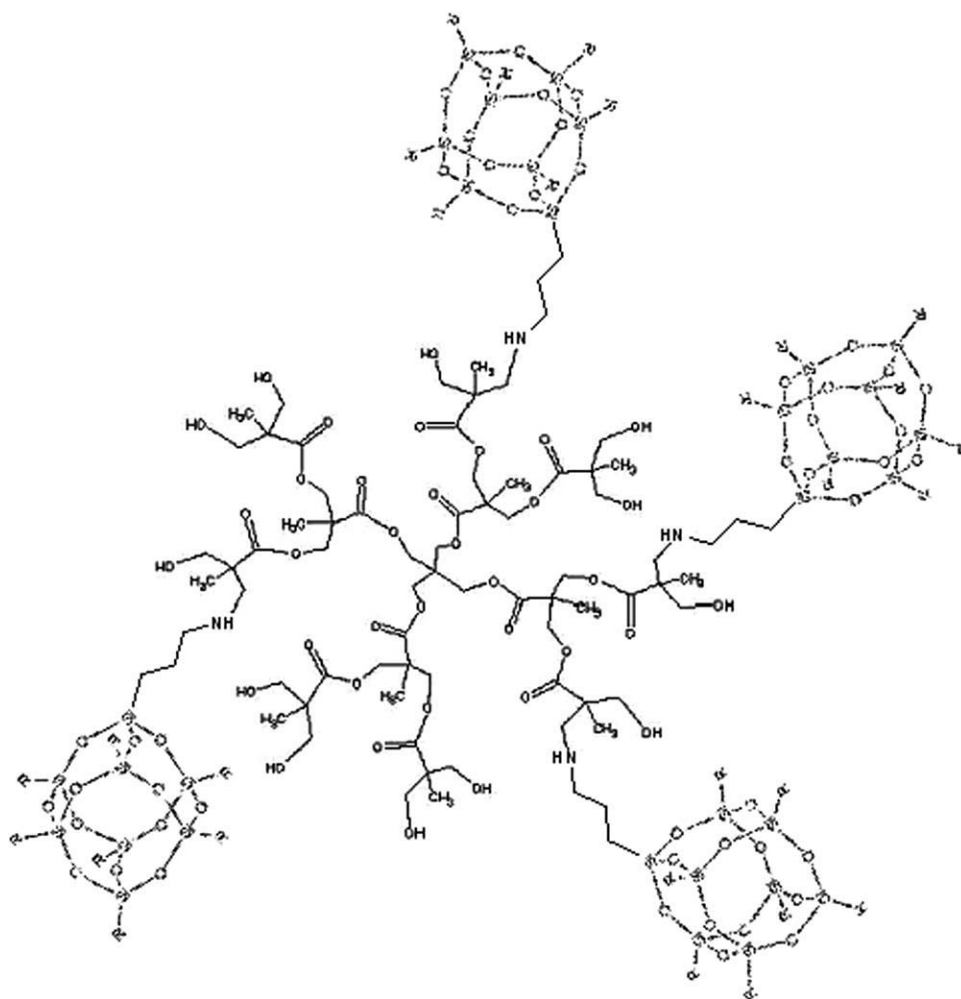


Figure 1 POSS-functionalized Boltorn H20.

$$\text{For } 1 < \text{slope} < 3 \quad \text{slope} = D_f \quad (2)$$

$$\text{For } 3 < \text{slope} < 4 \quad \text{slope} = 6 - D_f \quad (3)$$

Thermal analysis

A Perkin-Elmer TGA-7 thermogravimetric analyzer was used to analyze the thermal stability of the nanocomposites. Samples of ~ 10 mg were heated to 850°C at $20^\circ\text{C min}^{-1}$ in an inert environment provided by a 20 mL min^{-1} nitrogen purge. The mass loss and its derivative were recorded as a function of temperature.

Thermomechanical analysis

Stress-strain. An Instron Universal Testing Instrument, Model 4465 with 5 kN load cell was used to perform stress-strain analysis using dumbbell-shaped test bars according to ASTM D638-97, specimen type IV. A strain rate of 50 mm min^{-1} was applied to each sample at ambient temperature (30°C) to determine the linear viscoelastic region and elastic modulus. Results presented are the average of five measurements.

Creep recovery. Creep recovery was performed using a TA Instruments Q800 Dynamic Mechanical Analyzer. Test specimens displaying average dimensions of $\sim 10.00 \times 5.50 \times 0.80 \text{ mm}^3$ were subjected to an applied stress of 0.5 MPa for 20 min, followed by a recovery period of 80 min with 0.01 MPa applied stress. The applied stress chosen was within the linear viscoelastic region of all polymer films. Tests were conducted at 30°C , and all results presented are the average of triplicate measurements. The four-element model of Maxwell and Kelvin-Voigt (Fig. 2) was used to interpret the creep component. The springs correspond to elastic sections with moduli E_1 and E_2 , while the dashpots represent the viscosity (η_1 , η_2). The overall deformation of the model is given in eq. (4).

$$\varepsilon(f) = (\sigma_0/E_1) + (\sigma_0/\eta_1) + (\sigma_0/E_2)(1 - e^{-t/(\eta_2/E_2)}) \quad (4)$$

The stretched exponential function of Kohlrausch, Williams and Watts¹⁷ (KWW) was used to interpret the recovery behavior and is given in eq. (5);

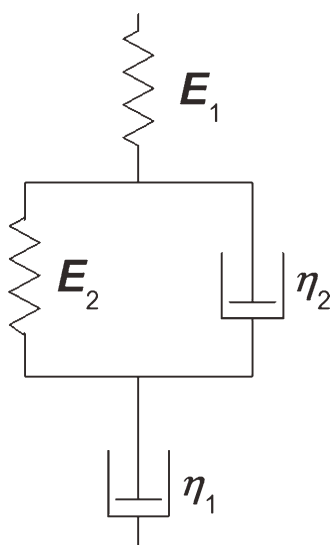


Figure 2 The four-element model.

$$\phi = A \exp^{-(t/\tau)^\beta} \quad (5)$$

where A is the pre-exponential coefficient, t is time, τ is the retardation time, and β is the nonlinearity coefficient ($0 < \beta < 1$).

Modulated force-thermomechanometry. mf-TM analysis was performed using a Perkin Elmer Diamond DMA with test specimens displaying average dimensions of $\sim 10.00 \times 5.50 \times 0.80 \text{ mm}^3$. Single frequency temperature scans were conducted using a static force of 500 mN, modulated force of 100 mN, and frequency of 1 Hz. The storage modulus (E'), loss modulus (E''), loss tangent ($\tan \delta$), and associated T_g of the films were measured as a function of temperature from -80 to $+110^\circ\text{C}$ at a heating rate of 2°C min^{-1} .

Material nomenclature

The nomenclature of the PU-Boltorn-POSS nanocomposites is PU- x - y , where x corresponds to the Boltorn hyperbranched dendrimer (H20 or H40) and y corresponds to the concentration of POSS-functionalized Boltorn within the linear TPU (1, 5, and 10%-wt).

RESULTS AND DISCUSSION

Chemical structure of POSS-functionalized Boltorn

FTIR spectroscopy was used to characterize the structure of the chemical components and to confirm functionalization. The infrared spectra of amino-treated POSS and POSS-functionalized Boltorn are presented in Figure 3. The amino-treated POSS displays several bands characteristic of its structure; 1100 (Si—O—Si stretching), 1462 , 1400 , 1366 and 1328 cm^{-1} (CH_2 and CH_3 bending vibrations and deformation), 2950 , and 2868 cm^{-1} (CH_3 , CH_2 , and CH

vibrational stretching of isobutyl "R" groups). In addition, the lack of a broad peak at $\sim 3300 \text{ cm}^{-1}$ indicates the lack of hydroxyl (OH) groups and confirms successful amino treatment of the POSS. The spectrum of POSS-functionalized Boltorn H20 and Boltorn H40 displayed similar spectra, characteristic of their polyester structure; 3430 cm^{-1} (OH stretching vibrations) and 1733 cm^{-1} (C=O stretching vibrations). Several bands indicated the presence of the amino-treated POSS. The characteristic Si—O—Si band is clearly visible at 1100 cm^{-1} as well as the various bands corresponding to the alkyl groups on the isobutyl "R" compatibilizing molecules. The bands at 2950 , 2868 , and 1472 cm^{-1} corresponding to vibrational stretching of the POSS isobutyl "R" groups. The large band at 3388 cm^{-1} corresponds to the OH end groups on the Boltorn dendrimer. This suggests that interaction between the hyperbranched dendrimer and POSS has occurred at some, though not all, hydroxyl groups. The benefit in retaining several OH groups is that they provide an affinity between the Boltorn dendrimer and polar groups within linear TPU.

Morphology

Scanning electron microscopy

The scanning electron microscope images of selected PU-POSS-Boltorn blends are displayed in Figure 4. Blends containing 1% wt POSS-functionalized Boltorn displayed an even distribution of hyperbranched dendrimer, with nonevident aggregation. As the concentration increased to 5%-wt, POSS agglomerates remained. Figure 4(a,b) displays several instances of clustering due to interactions between the POSS molecules, with agglomerates displaying average diameters of $\sim 30 \mu\text{m}$. This was

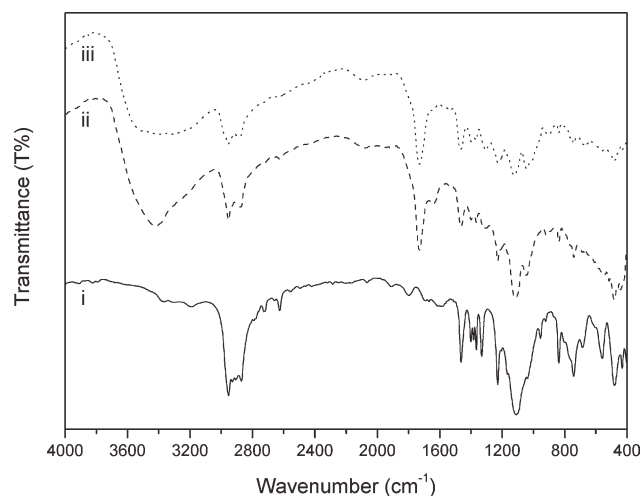


Figure 3 FTIR spectra; (i) amino-treated isobutylPOSS, (ii) functionalized Boltorn H20, and (iii) functionalized Boltorn H40.

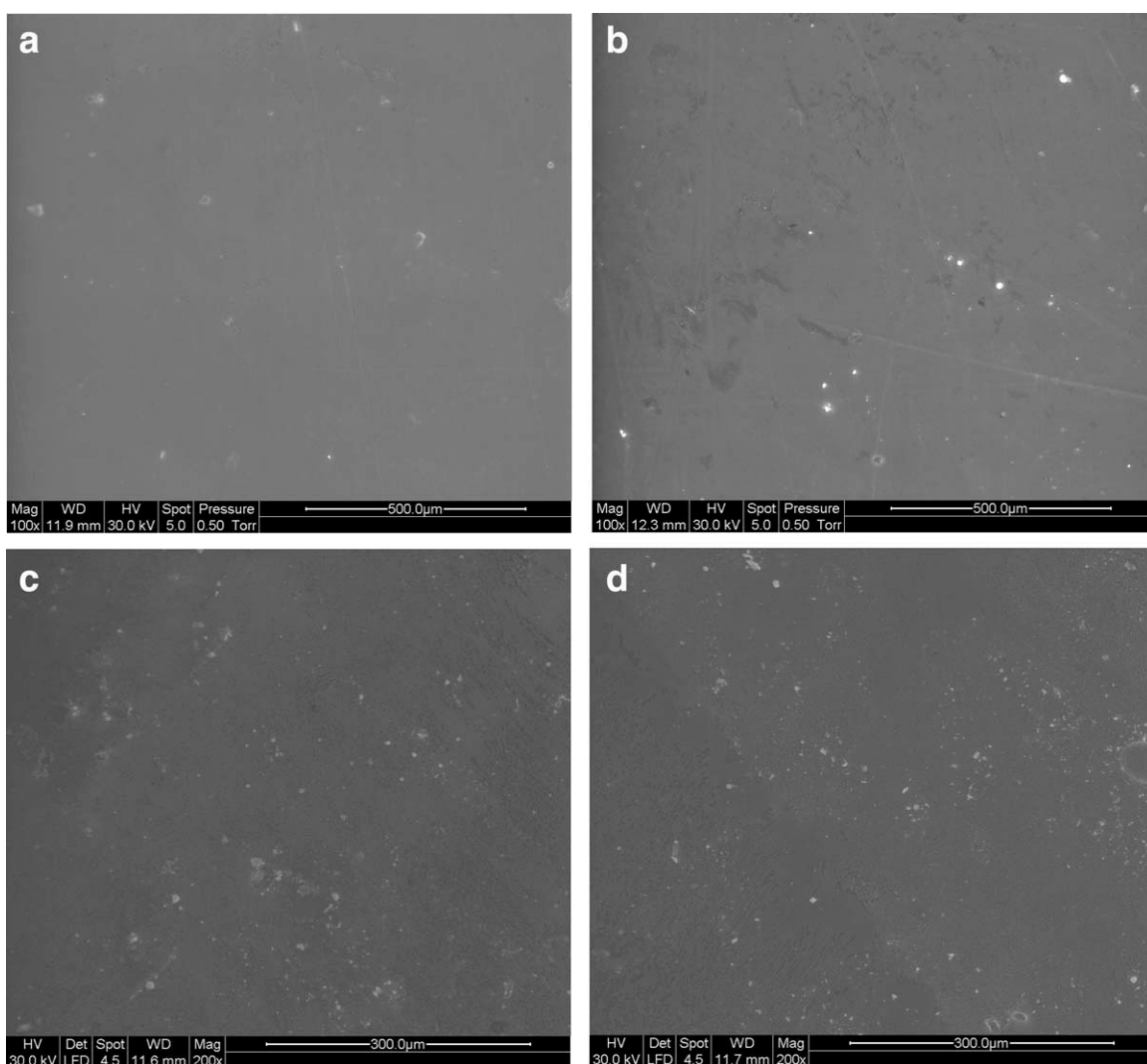


Figure 4 Scanning electron microscopy images of PU-POSS-Boltorn blends; (a) PU-H20 5, (b) PU-H40 5, (c) PU-H20 10, and (d) PU-H40 10.

facilitated due to the difference in polarity between the nonpolar POSS and polar hydroxyl groups on Boltorn and linear TPU. At Boltorn concentrations of 10%-wt [Fig. 4(c,d)], the frequency of agglomerates increased, due to the increased volume of POSS functional groups. However, the average agglomerate diameter remained at $\sim 30 \mu\text{m}$. No distinction in agglomerate dimension or frequency was observed for Boltorn H20 and Boltorn H40 blends. The unreacted hydroxyl groups on the Boltorn hyperbranched polyesters are available to interact with the linear TPU matrix. The specific interactions between the Boltorn and TPU provide a bridge/link between the linear polyurethane and the POSS end groups.

Small angle X-ray scattering

Figure 5 presents the one-dimensional SAXS profiles of the PU-POSS-Boltorn blends, while the data obtained from SAXS analysis are summarized in Ta-

ble I. The relative intensity was plotted against the scaling vector (q) magnitude. Pure TPU displayed a scattering profile with two maxima; a primary peak at $q = 0.01428 \text{ nm}^{-1}$ and shoulder at $q = 0.1949 \text{ nm}^{-1}$. The maxima correspond to the respective soft and hard segments that are characteristic of TPU structure. The incorporation of POSS-functionalized Boltorn diminished peak intensity, causing primary peaks to become broader and tapered. At dendrimer loadings of 10%-wt, the distinction between the soft and hard segment maxima is reduced, with PU-H20 10 and PU-H40 10 displaying scattering profiles with one broad maximum. Fu et al.¹⁸ related the reduction in scattering intensity in polyurethane to a break down or reduction of hard segments. In the case of the PU-POSS-Boltorn blends, the weaker peak intensities can be attributed to an increase in polyester (soft segment) content with the addition of the Boltorn aliphatic polyester, causing reduced scattering between the hard and soft segments.¹⁹ This

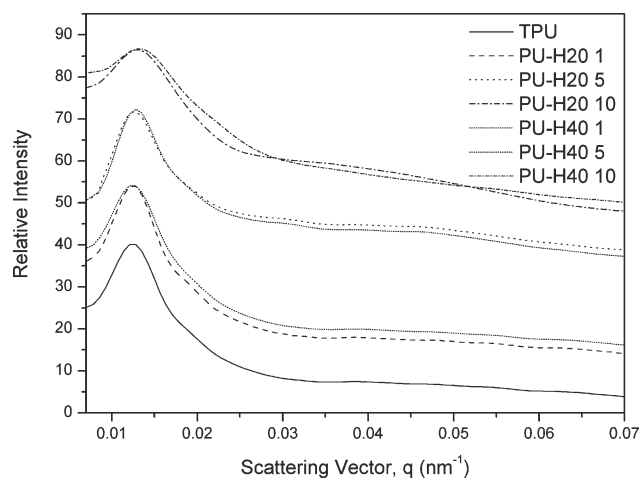


Figure 5 One-dimensional SAXS profiles of PU-POSS-Boltorn blends. Spectra have been shifted for clarity.

also accounts for the diminished hard segment shoulder at higher blend concentrations. In addition, several authors^{20,21} have reported reduced scattering intensity with increasing crosslink density. Crosslinks are known to restrict packing ability, “freezing” the morphology and preventing microphase separation.²² The diminished scattering peaks of the blends indicate that Boltorn may entangle and interpenetrate linear TPU chains, displaying behavior similar to a physical crosslink.

TPU exhibited a d -spacing value of 503 nm, determined from the maximum of the primary peak by $d = 2\pi/q_{\max}$. The incorporation of POSS-Boltorn hybrid dendrimer shifted the primary peak maximum to higher q values. Consequently, 10%-wt blends displayed the lowest d -spacing values of 483 (PU-H20 10) and 477 nm (PU-H40 10). Increased q or reduced d -spacing values in polyurethanes have been associated with enhanced miscibility and reduced phase size.^{22,23} The similar chemical structure of TPU and Boltorn promotes compatibility between the macromolecules. This enables the polyester arms of Boltorn to entangle throughout the soft segments within linear TPU, reducing unoccupied volume and making the polymer structure more compact and less mobile.²⁴ Figure 6 displays a proposed model of how POSS-functionalized Boltorn

TABLE I
SAXS Data of PU-POSS-Boltorn Blends

Material	d -Spacing (nm)	R_g (nm)	D_f
TPU	503	13.0	2.14
PU-H20 1	496	12.0	2.36
PU-H20 5	491	9.8	2.44
PU-H20 10	483	8.5	2.68
PU-H40 1	490	11.5	2.41
PU-H40 5	487	9.6	2.58
PU-H40 10	477	8.2	2.84

interacts with linear TPU. Boltorn H40 blends displayed lower d -spacing values than their H20 counterparts. This was due to the structure and large dimensions of Boltorn H40 that enable greater interaction and restrictions on TPU chains. Furthermore, POSS has been observed to reduce phase separation within polyurethane.^{18,25–27}

The radii of gyration (R_g) of the linear TPU hard segment within the blends were determined by constructing Guinier plots, as shown in Figure 7, while the values are summarized in Table I. Plotting $\ln(I)$ versus q^2 gave a linear graph from which R_g can be determined using eq. (1). The addition of functionalized Boltorn caused R_g to decrease, ranging from 13.0 nm (TPU) to 8.5 (PU-H20 10) and 8.2 nm (PU-H40 10). One probable explanation for this behavior can be related to the observed reduction in d -spacing values with increasing functionalized-Boltorn concentration. Romiszowski and Sikorski²⁸ studied the effects of confinement on linear and branched polymers, observing a reduction in R_g as the polymer became more confined and compact. The behavior was attributed to the polymer chains changing their structure from three-dimensional to a flat, two-dimensional conformation. Incorporation of POSS-functionalized Boltorn into linear PU reduced phase separation and created a more compact structure. This was indicative of the reduction in d -spacing values, suggesting the hard domains are closer together than in pure TPU. The effects of confinement and reduced unoccupied volume can lead to the domains



Figure 6 Distribution of POSS-functionalized Boltorn throughout the soft (polyester) segment within TPU.

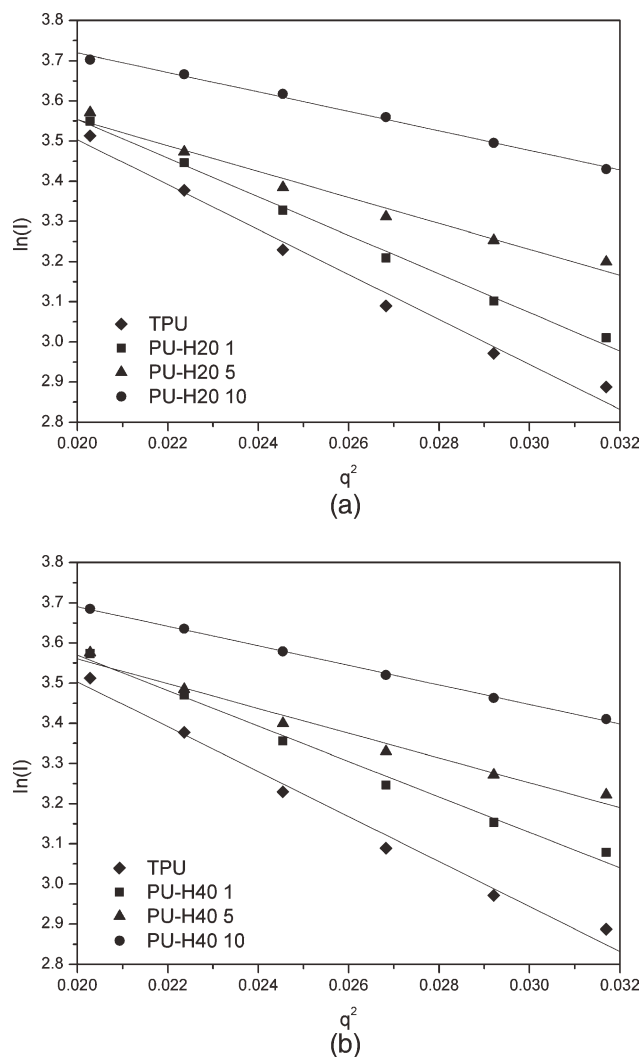


Figure 7 Guinier plots of PU-POSS-Boltorn blends; (a) Boltorn H20 blends and (b) Boltorn H40 blends.

becoming “flatter” in dimension, causing R_g to decrease. Boltorn H40 blends exhibited the lowest R_g values due to the greater influence on chain motion and larger occupied volume for which these dendrimers are responsible. Several authors^{29–31} have documented the relationship between molecular weight and R_g of branched polymers, observing reduced R_g values as M_w of the hyperbranched polymer increases. This relationship is in agreement with comparisons of Boltorn H20 and H40 blends; however, it should be noted that polyurethane hard domains are the primary contributors to scattering.

Porod plots were constructed by plotting $\log(I)$ versus $\log(q)$ to give a linear graph. Using the slope and eq. (2), the fractal dimension (D_f) of blends was determined. The Porod plots are shown in Figure 8 while the D_f values are presented in Table I. Pure TPU displayed a D_f value of 2.14. The addition of POSS-functionalized Boltorn into the matrix increased D_f values, with PU-H20 10 and PU-H40 10

displaying maximum values of 2.68 and 2.84, respectively. D_f values between 2 and 3 are characteristic of mass fractal structures, such as polymer networks. All blends exhibited D_f values between 2 and 3, that is typical for branched polymers and confirms that the blends maintain a mass fractal geometry. The increased fractal dimensionality is indicative of a more compact chain structure³² and is anticipated for linear-hyperbranched polymer blends.³³ As Boltorn concentration is increased, the total number of contact points between the dendrimer and linear chain is enhanced.³⁴ Increasing dendrimer size or dimension has a similar effect; hence the Boltorn H40 blends displayed larger D_f values than those containing Boltorn H20. The observations are in agreement with the reduced R_g and confirm interaction and entanglement of Boltorn and TPU chains. Furthermore, the SAXS data indicate that morphology of the blends is primarily dictated by the Boltorn dendrimer, with minor contributions from POSS.

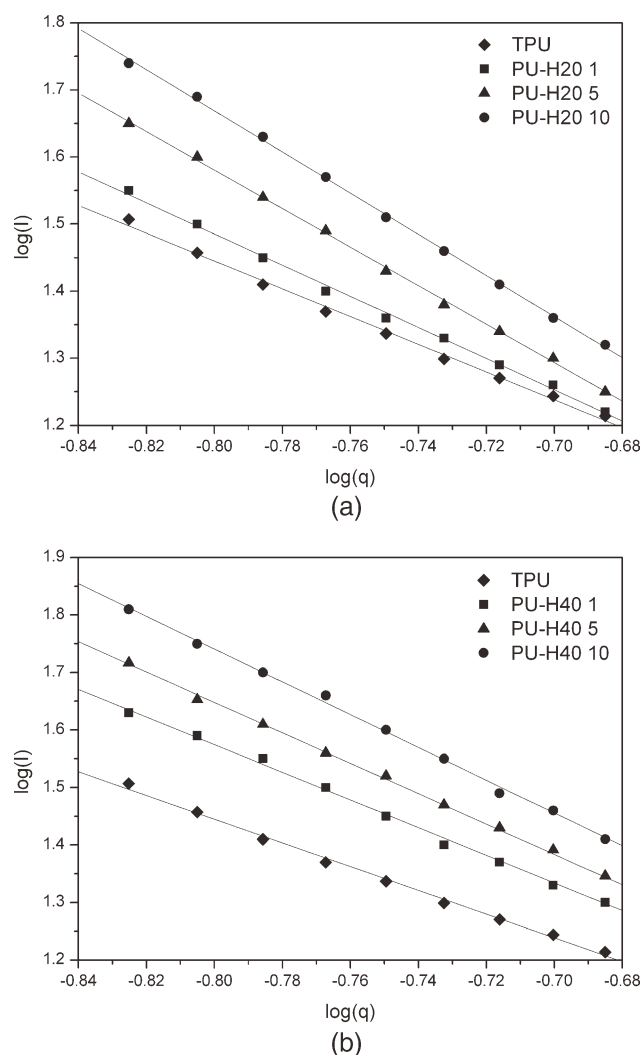


Figure 8 Porod plots of PU-POSS-Boltorn blends; (a) Boltorn H20 blends and (b) Boltorn H40 blends.

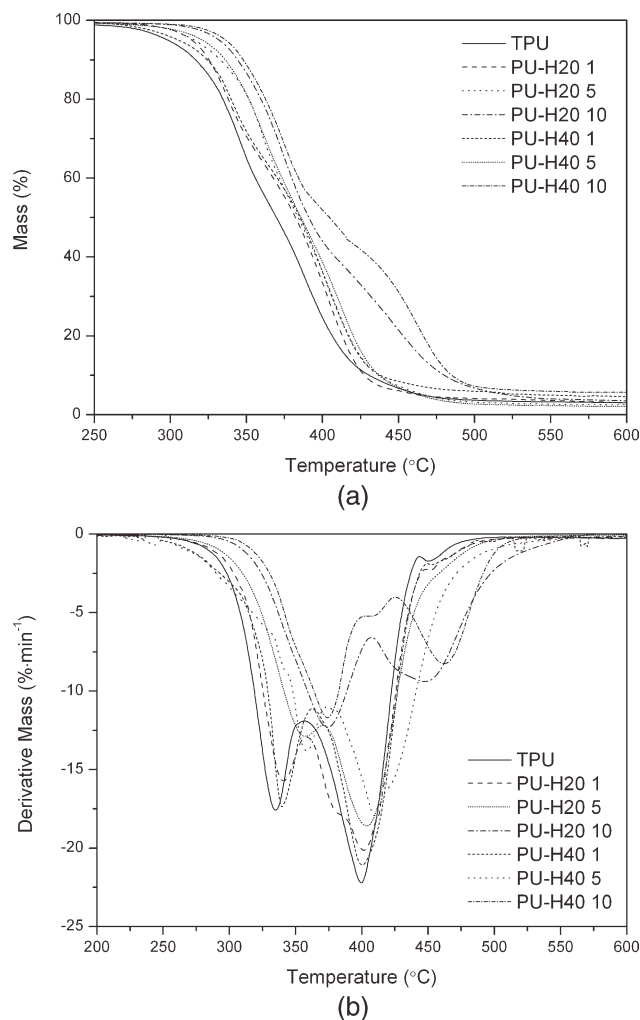


Figure 9 TGA curves of PU-POSS-Boltorn blends; (a) mass loss and (b) derivative mass.

Thermal stability

The mass loss curves of TPU and PU-POSS-Boltorn blends are presented in Figure 9(a). Pure TPU experienced thermal degradation in two steps, corresponding to decomposition of the hard (first step) and soft (second step) segments. The first step involves depolycondensation,³⁵ resulting in the formation of isocyanate, alcohols, primary or secondary amines, olefins, and carbon dioxide.³⁶ In the second step, isocyanates are dimerized to carbodiimides, which react with alcohol groups to form stable substituted ureas.³⁷ The addition of POSS-functionalized Boltorn increased the thermal stability of the blends, with curves shifting toward higher temperatures and reaching maximum values at filler loadings of 10%-wt. Blends containing 5 and 10%-wt Boltorn H40 exhibited greater thermal stability properties than their Boltorn H20 counterparts for equal concentrations. Similar results were reported by Vukovic et al.,³⁸ who observed that thermal stability of hyperbranched polyesters increased with genera-

tion. The enhanced thermal properties were attributed to an increase in molar mass³⁹ and greater number of —OH end groups. The more numerous hydroxyl end groups allow for a greater degree of specific interactions between (a) the linear and hyperbranched polymers and (b) between the dendrimers. This retards molecular vibrations and rotation that occurs at the onset of thermal degradation. In addition, the greater number of POSS bonded to Boltorn H40 provide a greater contribution to thermal stability than those bonded to Boltorn H20.

As shown in the derivative mass loss curves [Fig. 9(b)], pure TPU exhibited two T_d values of 335 and 399°C, for the first and second degradation steps, respectively. The addition of functionalized Boltorn H20 increased T_d values, ranging from 341 and 401°C (PU-H20 1) to 372 and 442°C (PU-H20 10). Similar trends were observed for blends containing Boltorn H40, with T_d values increasing from 340 and 400°C (PU-H40 1) to 374 and 459°C (PU-H40 10). Blends displayed lower mass loss rates, with the rate decreasing as Boltorn concentration increased. This is indicative of the increase in thermal stability and confirms that the functionalized dendrimers decrease the rate of thermal degradation within polyurethane.

The thermal stability of PU is dependent on several factors, including hard segment volume, chain extender volume/type, and the diisocyanate type.⁴⁰ The addition of fillers or blending with other polymers can additionally influence thermal properties. Dendritic polyesters have been shown to exhibit superior thermal stability to linear counterparts,³⁸ due to their unique architectural structure. The incorporation of Boltorn into a polyurethane matrix results in intra/intermolecular bridges between the linear and dendritic polymers via hydroxyl groups. These interactions restrict molecular vibrations and rotations that occur when thermally excited,³⁶ increasing thermal stability. The enhanced thermal behavior correlates with results obtained by Maji and Bhowmick,²⁶ who prepared polyurethanes with Boltorn crosslinks. The polymers exhibited increased thermal stability, attributed to increased molecular weight and polyurethane-Boltorn interactions. During thermal degradation, polymer chains must break-up/debond into smaller segments to allow for elimination of parts of the structure. Increasing the cross-link density or molecular weight results in materials fragmenting into larger segments than otherwise. These larger polymer segments require more energy to break into portions small enough to be eliminated, exhibiting increase thermal stability in the process.

In addition to Boltorn, the inorganic structure of POSS leads to the molecule exhibiting a high-intrinsic thermal stability. A number of mechanisms have

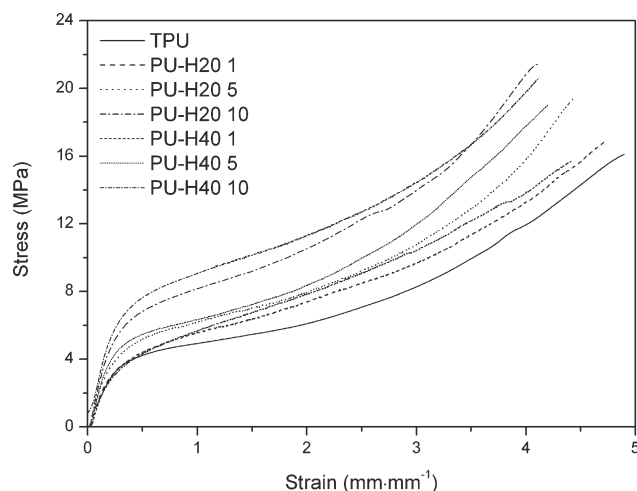


Figure 10 Stress–strain curves of PU-POSS-Boltorn blends.

been proposed to explain how POSS improves thermal stability in polymer composites. One possible explanation is that POSS restrict polymer chain motions, due to polymer–filler interactions or by the large inertia exhibited by segments of polymer containing POSS.^{41,42} Alternatively, polymer segments near POSS molecules may degrade more slowly due to the POSS providing heat shielding and the “most torturous path” for the elimination of degradation products. The results indicate that Boltorn and POSS provide a synergistic effect in increasing the thermal stability of TPU, a valuable attribute.

Thermomechanical analysis

Stress–strain analysis

The stress–strain curves of PU-POSS-Boltorn blends are presented in Figure 10, while the stress–strain data are summarized in Table II. Pure TPU displayed a tensile modulus (E) of 15.32 MPa and break stress of 16.13 MPa. The incorporation of POSS-functionalized Boltorn had a positive effect on E , with values increasing from 15.98 (PU-H20 1) to 20.24 MPa (PU-H20 10) in materials blended with Boltorn H20. Similar results were observed for Boltorn H40 blends, with E values ranging from 15.53 (PU H40 1) to 24.62 MPa (PU-H40 10). Accompanying the enhanced tensile modulus was an increase in break strength with functionalized Boltorn concentration, reaching maximum values of 21.40 (PU-H20 10) and 20.57 MPa (PU-H40 10).

In linear-dendritic polymer blends, enhancement of mechanical properties will occur if (a) entanglements are present, (b) if the dendrimer possess a rigid structure due to the presence of aromatics, or (c) if it is crystalline.^{43,44} Both the first two factors can be applied to the PU-POSS-Boltorn blends. First,

unreacted hydroxyl end groups on the Boltorn hyperbranched polyester provide compatibility with the linear TPU, leading to hydrogen bonding between the linear and dendritic polymer chains. These interactions encourage the hyperbranched dendrimers to entangle throughout the linear TPU chains, creating a restriction in segmental motion. Second, the presence of POSS provides inherent rigidity to the Boltorn structure, providing additional restrictions on chain motion. A consequence of the increased rigidity and segmental restrictions was the decrease in elongation at break, with 10%-wt blends displaying the least-elastic behavior. Furthermore, the intrinsic strength of POSS allows it to absorb applied stress. This is facilitated by Boltorn acting as a “compatibilizer” or “bridge” between the TPU and POSS, allowing stress to be transferred from the former to the latter.

Differences in static mechanical properties were observed for Boltorn H20 and Boltorn H40 blends, particularly in tensile modulus and elongation at break. Films containing Boltorn H40 displayed larger tensile moduli and were more brittle than their Boltorn H20 counterparts, especially at concentrations of 5 and 10%-wt. This observation correlates with the results presented by Maji and Bhowmick.²⁶ They observed that increasing the dendrimer generation increased E values and reduced elasticity in polyurethane-Boltorn blends. The enhanced moduli values were attributed to the increased functionality (number of $-OH$ end groups) in higher generation Boltorn polyesters. Boltorn H40 theoretically has 64 primary hydroxyl groups, compared to 16 on Boltorn H20,⁴⁵ allowing for greater linear-dendritic polymer interaction and further restrictions on chain mobility. The reduction in elasticity was attributed to shorter segments of linear TPU chain between Boltorn dendrimers, which become smaller with increased Boltorn concentration and dendrimer generation. As chain segment length decreases, so does the maximum length which the uncoiled chains can be extended to under applied stress. This increases the brittleness of the material and promotes the earlier onset of failure.

TABLE II
Stress–Strain Data of PU-POSS-Boltorn Blends

Material	Tensile modulus (MPa)	Break stress (MPa)	Elongation at break (mm mm ⁻¹)
TPU	15.32	16.13	4.9
PU-H20 1	15.98	16.87	4.7
PU-H20 5	17.83	19.38	4.3
PU-H20 10	20.24	21.40	4.1
PU-H40 1	15.53	15.71	4.4
PU-H40 5	19.16	19.05	4.2
PU-H40 10	24.62	20.57	4.1

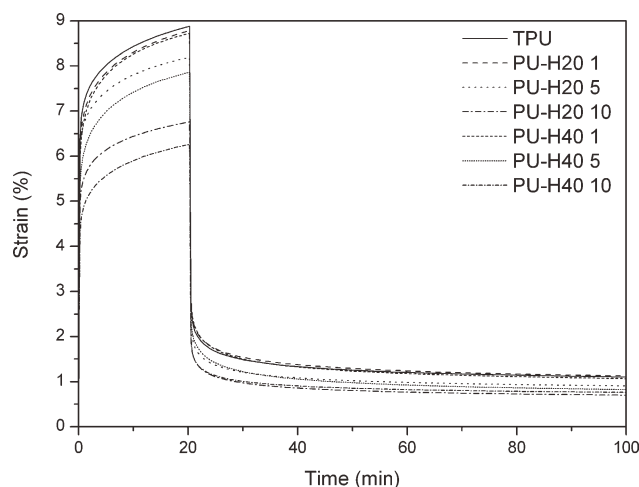


Figure 11 Creep-recovery curves of PU-POSS-Boltorn blends.

Creep-recovery analysis

The creep-recovery curves of the PU-POSS-Boltorn blends are displayed in Figure 11. Increasing the POSS-functionalized Boltorn concentration decreased creep deformation. This indicates that linear polyurethane chain motions are suppressed during applied load. The results correlate with those obtained from stress-strain analysis and can be attributed to the influence of Boltorn and POSS. First, the Boltorn hyperbranched polyesters are able to interact with the linear TPU chains, restricting segmental motions. Second, the rigid POSS impart stiffness and reduced ductility into the polymer matrix. As observed in the stress-strain data, blends containing Boltorn H40 displayed greater resistance to creep deformation than their Boltorn H20 counterparts, particularly at concentrations of 5 and 10%-wt. This was due to the greater number of OH end groups on Boltorn H40, which provide the dendrimer more sites to interact with the linear TPU matrix. Furthermore, the segments of linear PU chain between dendrimers are shorter for Boltorn H40 blends than those containing Boltorn H20, causing a reduction in elastic behavior.

Table III summarizes the four-element model parameters calculated to interpret the creep behavior

of the blends. Pure TPU displayed the greatest strain response to applied load. Blends displayed a reduced creep response, providing restrictions to both elastic and viscous components of the model. The Maxwell modulus (E_1) increased with Boltorn content, confirming the POSS-dendrimer hybrids effect flow properties of linear TPU. Similarly, the Maxwell (η_1) viscosity increased with blend concentration, confirming resistance to deformation. Blends containing Boltorn H40 exhibited larger Maxwell component (E_1 and η_1) values than their Boltorn H20 counterparts, reflecting restricted uncoiling and intermolecular slippage. Unrecovered strain was observed for all materials, due to chain slippage and detachment of hard segments from the soft segments that occur during deformation. Increasing the dendrimer concentration resulted in greater permanent deformation, due to chain relaxation being hindered by Boltorn and POSS. This leads to irreversible chain slippage. Consequently, the reversible Voigt viscosity (η_2) increased with blend concentration, indicating a decrease in the likelihood of TPU chain uncoiling.

The retardation time (t) is the time required for the Voigt element (viscoelastic component) to recover to 63.21% (or $1 - 1/e$) of its total deformation. It is needed to calculate η_2 and was obtained using eq. (4). Blends displayed lower t as dendrimer content was increased, suggesting an increase in solid-like behavior. Similarly, recovery curves became flatter with increasing blend concentration, indicating the viscoelastic and elastic components experience faster recovery. Boltorn H40 blends exhibited shorter retardation times than those containing Boltorn H20; indicative of the influence dendrimer generation has on recovery and static mechanical properties. The calculated parameters accurately represent experimental data observed in the creep component and stress-strain analysis.

The KWW stretched exponential function was applied to the blends to interpret the recovery component. The results are summarized in Table IV. The pre-exponential constant (A) and relaxation time decreased with increasing blend concentration, corresponding to reduction in molecular mobility. The

TABLE III
Creep-Recovery Data of PU-POSS-Boltorn Blends

Material	E_1 (MPa)	η_1 (MPa s ⁻¹)	E_2 (MPa)	η_2 (MPa s ⁻¹)	τ (min)	Permanent deformation (%)
PU	0.42	18.04	0.10	1.58	15.80	10
PU-H20 1	0.45	22.12	0.11	1.63	14.82	11
PU-H20 5	0.56	28.59	0.18	2.12	11.77	11
PU-H20 10	0.63	30.82	0.26	2.23	8.58	12
PU-H40 1	0.49	20.58	0.13	1.67	12.85	10
PU-H40 5	0.64	32.89	0.17	2.17	12.77	12
PU-H40 10	0.74	37.13	0.24	2.20	9.17	13

TABLE IV
KWW Parameters of PU-POSS-Boltorn Blends

Material	A	β	τ (s)
TPU	5.33	0.12	6.40
PU-H20 1	5.48	0.10	6.23
PU-H20 5	6.77	0.10	5.93
PU-H20 10	10.37	0.09	4.11
PU-H40 1	6.84	0.10	6.34
PU-H40 5	7.52	0.11	4.83
PU-H40 10	8.56	0.10	2.47

reduced relaxation time confirms the increase in solid-like behavior with blend concentration and is in agreement with both the experimental creep component and four-element model parameters. Correspondingly, the shape fitting parameter β decreased with Boltorn content, indicating an increase in co-operative segmental motions. These observations strongly indicate that Boltorn and POSS impart considerable influence on the flow of linear TPU, the results of which extend to the mechanical-property response.

Modulated force-thermomechanometry

The storage moduli (E') of PU-POSS-Boltorn blends are presented in Figure 12 while E' values are summarized in Table V. Pure TPU displayed an E' value of ~ 2.5 GPa at -80°C . The addition of 1%-wt functionalized Boltorn had marginal impact on the storage modulus, resulting in E' values remaining at ~ 2.5 GPa. Increasing the POSS-dendrimer hybrid concentration increased the storage modulus, with PU-H20 5 and PU-H20 10 displaying E' values of ~ 2.8 and 3.3 GPa, respectively, at -80°C . Similar behavior was observed for blends containing Boltorn H40, with maximum modulus values recorded for PU-H40 10 (~ 3.8 GPa at -80°C). The larger E' val-

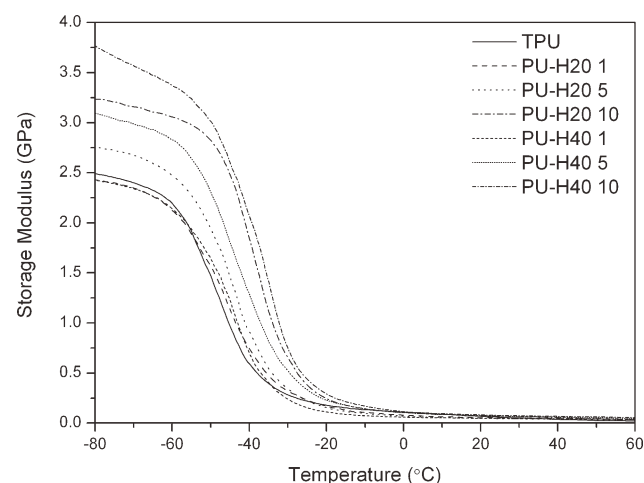


Figure 12 Storage (E') moduli of PU-POSS-Boltorn blends.

TABLE V
mf-TM Data of PU-POSS-Boltorn Blends

Materials	E'' peak T_g ($^\circ\text{C}$)	Tan δ peak T_g ($^\circ\text{C}$)	E' at -80°C
TPU	-47	-31	2.5
PU-H20 1	-45	-28	2.5
PU-H20 5	-43	-26	2.8
PU-H20 10	-37	-20	3.3
PU-H40 1	-45	-28	2.4
PU-H40 5	-41	-25	3.1
PU-H40 10	-35	-19	3.8

ues indicate an increase in material strength with POSS-Boltorn content and correlate with stress-strain data. This increase in mechanical strength is facilitated by the restricted chain mobility and enhanced rigidity that were imparted by the Boltorn and POSS, respectively. Boltorn H40 blends displayed larger E' values than their Boltorn H20 counterparts for equal concentrations. This was attributed to the influence of dendrimer size and number of functional groups on mechanical properties,²⁶ with blends displaying trends similar to those observed in stress-strain analysis.

Figure 13 displays the loss (E'') moduli of the blends while T_g values are summarized in Table V. Pure TPU displayed a T_g of -47°C . Increasing the blend concentration had a positive effect on the T_g , reaching maximum values of -37°C (PU-H20 10) and -35°C (PU-H40 10). This behavior is in agreement with literature,^{46,47} attributing the increased T_g in linear-dendrimer blends to reduced free volume and restrictions imparted by the hyperbranched macromolecules on linear chain motions. These restrictions are usually facilitated through hydrogen bonding between the linear and dendritic polymers, causing an antiplasticizing effect. Within the PU-POSS-Boltorn blends, these hydrogen bonds can

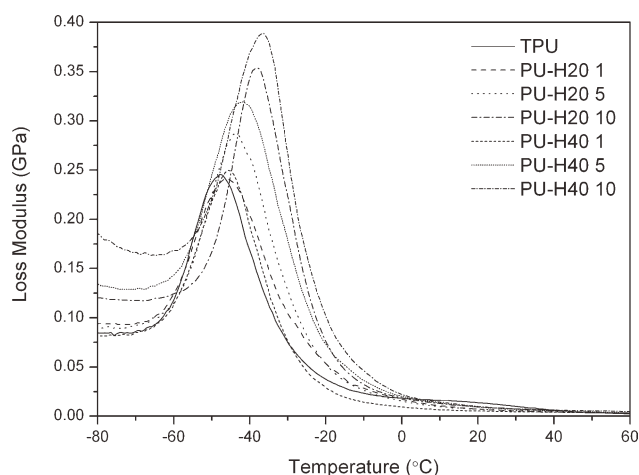


Figure 13 Loss (E'') moduli of PU-POSS-Boltorn blends.

occur through the unreacted OH groups on Boltorn and C=O groups on the polyester (soft segment) component of linear TPU, increasing mechanical and T_g properties. Furthermore, the T_g of Boltorn (31°C)⁴⁵ is considerably higher than linear TPU (-47°C), allowing the dendrimer to remain solid-like and interact with linear chains while they experience T_g and eventually flow.⁴⁸ The rigid structure of POSS is also widely known to impart restrictions on polymer chains and increase the T_g of polyurethane.^{49–53} All blends displayed a single loss peak, corresponding to the T_g of linear TPU. This confirms that Boltorn dendrimer is miscible with TPU's soft, polyester segments (refer Fig. 6). In addition, the single maximum strongly suggests that functionalized Boltorn is primarily distributed throughout the soft segment within TPU.

The addition of POSS-functionalized dendrimer increased the breadth of the E'' curves, with 10% wt blends displaying the broadest peaks. This indicates the blends experienced glass-rubber transition across a broader temperature range, with the POSS-Boltorn hybrid subsequently increasing the segmental relaxation time of the linear polyurethane matrix. Blends containing Boltorn H40 displayed higher T_g values than those composed of Boltorn H20, particularly at concentrations of 5 and 10% wt. Furthermore, Boltorn H40 blends yielded wider E'' curves. These results correlate with the observations of Carr et al.⁴⁷ and Xu et al.,⁴⁶ who reported an increase in T_g values with dendrimer size in linear-dendrimer blends. They attributed the behavior to increased chain entanglement density in blends containing larger dendrimers, shifting T_g toward higher temperatures. The more numerous hydroxyl groups on Boltorn H40 allow for an increased degree of interaction between the dendrimer and linear polymer, increasing the total amount and extent of chain restrictions. In addition, the large size of Boltorn H40 (compared to Boltorn H20) reduces the length of linear TPU chain segments between dendrimers, reducing the degree of rotation the segment can experience.

The loss tangent ($\tan \delta$) of the blends is presented in Figure 14. As with the E'' curves (refer Fig. 13), a single peak is observed confirming adequate TPU-Boltorn interaction. The T_g values obtained from the loss tangent maximum were ~16–17°C higher than those obtained from the E'' curve maxima. However, trends displayed in the $\tan \delta$ curves were similar to those in the loss modulus, with T_g increasing with blend concentration and Boltorn H40 blends displaying the largest shift in T_g . The addition of Boltorn caused a reduction in peak height, indicative of diminished damping ability. The dampening properties of a polymer become greater as the number of chain movements is increased. The incorporation of POSS and Boltorn reduces the number of chain

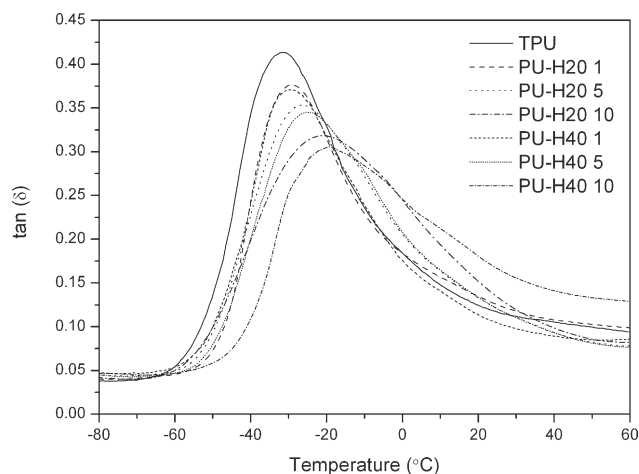


Figure 14 Loss tangent ($\tan \delta$) of PU-POSS-Boltorn blends.

motions and free volume, causing a reduction in damping. The thermomechanical data showed that Boltorn H40 blends experienced the least amount of chain movement. As a result, these materials displayed poorer damping properties than Boltorn H20 blends, indicative of the smaller $\tan \delta$ peaks.

CONCLUSION

Boltorn hyperbranched aliphatic polyesters were functionalized with amino-treated isobutylPOSS and blended with linear TPU. Functionalization was confirmed using FTIR. Agglomerate size and frequency amongst POSS increased with blend concentration, due to increased interparticle interaction. Blend morphology was primarily influenced by the Boltorn dendrimer, with minor contributions from POSS. The radius of gyration decreased and fractal dimensionality increased with functionalized dendrimer concentration. This indicated a reduction in free volume and increased compactness amongst polymer chains. Blends exhibited smaller d -spacing values, suggesting the Boltorn and POSS encourage enhanced miscibility and reduce phase separation.

Thermal stability increased with POSS-functionalized Boltorn content, due to restrictions on polymer chain vibration imparted by Boltorn and thermal shielding supplied by POSS. The tensile modulus and strength increased with blend concentration, while ductility decreased due to the rigid nature of the materials. Molecular restrictions imparted by the POSS-Boltorn hybrid reduced creep deformation and increased permanent strain with filler content. Storage modulus, loss modulus, and glass transition temperature increased with blend concentration. Blends containing Boltorn dendrimers with a higher generation exhibited superior thermal and

mechanical properties than those blended with lower generation Boltorn. This was attributed to the enhanced TPU-Boltorn interaction and restrictions imparted on linear polyurethane chains. Material properties were influenced by both the Boltorn dendrimer and POSS, indicating that blending with the functionalized hyperbranched macromolecule provides a viable method of enhancing the thermal and mechanical properties of TPU.

APPENDIX: CALCULATION OF THE NUMBER OF POSS MOLECULES BONDED TO A SINGLE BOLTORN DENDRIMER

FTIR absorbance spectra were used to determine the number of POSS molecules that reacted with hydroxyl groups on the Boltorn dendrimers following functionalization, as shown in Figure A1. Several

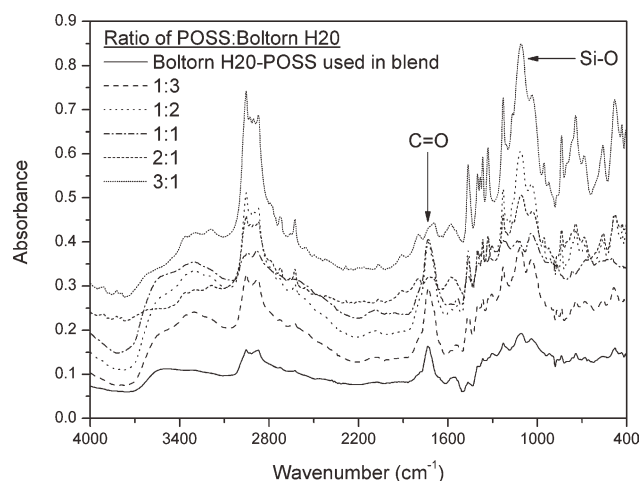


Figure A1 Absorbance spectra of POSS-functionalized Boltorn H20. Spectra have been shifted 0.05 U vertically for clarity.

POSS-functionalized Boltorn samples were prepared in different molar ratios as summarized in Table AI.

The ratio of the peak heights at $\sim 1720 \text{ cm}^{-1}$ (C=O stretching within Boltorn) and $\sim 1100 \text{ cm}^{-1}$ (Si-O stretching within POSS) was taken and plotted as a function of the molar ratio of POSS : Boltorn to yield a linear graph as shown in Figure A2.

Example calculation using POSS-functionalized Boltorn H20

Boltorn H20 displayed an absorbance peak ratio of 0.19 : 0.16 or 1.19. Substituting 1.19 into the linear fit equation obtained from Figure A1 yields a molar fraction of 0.72. This corresponds to a molar ratio of 1 : 1.4 (POSS : Boltorn). Using these molar values, the mass of Boltorn and POSS was determined using eq. (A1):

$$n = \frac{\text{mass}}{\text{molar mass}} \quad (\text{A1})$$

Boltorn H20:

$$1.4 = \text{mass}/2100$$

$$\text{Mass} = 2940 \text{ g}$$

POSS:

$$1 = \text{mass}/871.92$$

$$\text{Mass} = 871.62 \text{ g}$$

To determine the number of POSS molecules bonded to one Boltorn dendrimer, eq. (A2) was used:

$$\text{Number of molecules} = \frac{A_V}{(\text{mass} \times \text{molar mass})} \quad (\text{A2})$$

where A_V is Avagadro's number.

TABLE AI
Peak Intensity and Molar Ratios of POSS-Functionalized Boltorn Samples

Molar ratio (POSS : Boltorn)	Mole of POSS/mol of Boltorn (x -axis)	Peak height at $\sim 1100 \text{ cm}^{-1}$ (POSS peak)	Peak height at $\sim 1720 \text{ cm}^{-1}$ (Boltorn peak)	POSS peak/Boltorn peak (y -axis)
<i>POSS-functionalized Boltorn H20</i>				
1 : 3	0.33	0.39	0.40	0.98
1 : 2	0.5	0.39	0.37	1.05
1 : 1	1	0.39	0.29	1.35
2 : 1	2	0.48	0.25	1.92
3 : 1	3	0.69	0.28	2.46
<i>POSS-functionalized Boltorn H40</i>				
1 : 3	0.33	0.53	0.49	1.08
1 : 2	0.5	0.48	0.43	1.12
1 : 1	1	0.49	0.40	1.23
2 : 1	2	0.66	0.46	1.43
3 : 1	3	0.72	0.42	1.71
POSS-functionalized Boltorn H20 used in blends		0.19	0.16	1.19
POSS-functionalized Boltorn H40 used in blends		0.15	0.12	1.25

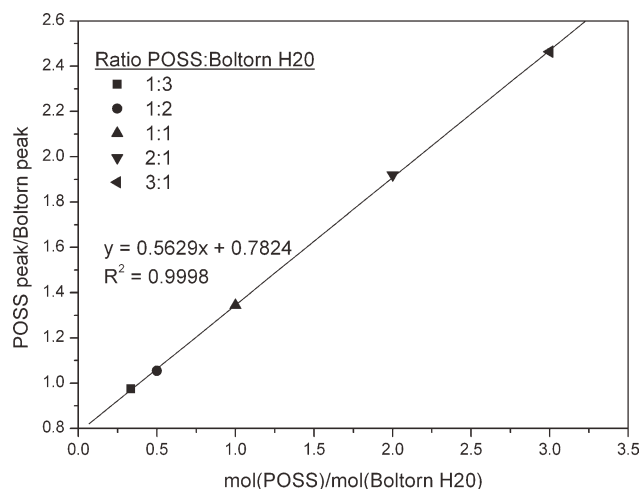


Figure A2 Linear plot of absorbance peak ratio versus molar ratio.

Boltorn H20:

$$\begin{aligned} \text{Number of molecules} &= 6.022 \times 10^{23} / (2940 \times 2100) \\ &= 9.75057 \times 10^{16} \end{aligned}$$

POSS:

$$\begin{aligned} \text{Number of molecules} &= 6.022 \times 10^{23} / (871.92 \times 871.92) \\ &= 7.92396 \times 10^{17} \end{aligned}$$

Number of Boltorn H20 molecules:

$$9.75057 \times 10^{16} / 9.75057 \times 10^{16} = 1$$

Number of POSS molecules:

$$7.92396 \times 10^{17} / 9.75057 \times 10^{16} = 8.1$$

~ 8 POSS molecules attached to 1 Boltorn H20 dendrimer.

Similarly, the molar ratio of POSS : Boltorn H40 was calculated to be 1 : 1, with ~ 31 POSS molecules attached to 1 Boltorn H40 dendrimer.

References

- Hult, A.; Malmström, E.; Johansson, M.; Sörensen, K. U.S. Pat.017,060 (1993).
- Zhang, X. *Polym Int* 2010, 60, 153.
- Pilla, S.; Kramschuster, A.; Lee, J.; Clemons, C.; Gong, S.; Turng, L. S. *J Mater Sci* 2010, 45, 2732.
- Czech, P.; Okrasa, L.; Boiteux, G.; Mechin, F.; Ulanski, J. *Proceedings of the first Workshop NanoFun-Poly, Dresden, Germany, 2005*; p 17–20.
- Czech, P.; Okrasa, L.; Méchin, F.; Boiteux, G.; Ulanski, J. *Polymer* 2006, 47, 7207.
- Okrasa, L.; Czech, P.; Boiteux, G.; Méchin, F.; Ulanski, J. *Polymer* 2008, 49, 2662.
- Ratna, D.; Varley, R.; Raman, R. K. S.; Simon, G. P. *J Mater Sci* 2003, 38, 147.
- Mezzenga, R.; Boogh, L.; Månson, J. A. E. *Compos Sci Technol* 2001, 61, 787.
- Oh, J. H.; Jang, J.; Lee, S. H. *Polymer* 2001, 42, 8339.
- Plummer, C. J. G.; Mezzenga, R.; Boogh, L.; Månson, J. A. E. *Polym Eng Sci* 2001, 41, 43.
- Plummer, C. J. G.; Garamszegi, L.; Leterrier, Y.; Rodlert, M.; Månson, J. A. E. *Chem Mater* 2002, 14, 486.
- Rodlert, M.; Plummer, C. J. G.; Garamszegi, L.; Leterrier, Y.; Grünbauer, H. J. M.; Månson, J. A. E. *Polymer* 2004, 45, 949.
- Fu, B. X.; Hsiao, B. S.; Pagola, S.; Stephens, P.; White, H.; Rafailovich, M.; Sokolov, J.; Mather, P. T.; Jeon, H. G.; Phillips, S.; Lichtenhan, J.; Schwab, J. *Polymer* 2001, 42, 599.
- DeArmitt, C.; Wheeler, P. *Plast Add Compound* 2008, 10, 36.
- Scott, D. W. *J Am Chem Soc* 1946, 68, 356.
- Sterescu, D. M.; Stamatialis, D. F.; Mendes, E.; Kruse, J.; Rätzke, K.; Faupel, F.; Wessling, M. *Macromolecules* 2007, 40, 5400.
- Williams, G.; Watts, D. C. *Trans Faraday Soc* 1970, 66, 80.
- Fu, B.; Zhang, W.; Hsiao, B.; Rafailovich, M.; Sokolov, J.; Johansson, J.; Sauer, B.; Philips, S.; Balinski, R. *High Perform Polym* 2000, 12, 565.
- Sarva, S. S.; Hsieh, A. J. *Polymer* 2009, 50, 3007.
- Trimmel, G.; Fratzl, P.; Schubert, U. *Chem Mater* 2000, 12, 602.
- Travas-Sejdic, J.; Easteal, A.; Knott, R.; Pedersen, J. S. *J Appl Crystal* 2000, 33, 735.
- Russell, T. P.; Lee, D. S.; Nishi, T.; Kim, S. C. *Macromolecules* 1993, 26, 1922.
- Aurilia, M.; Piscitelli, F.; Sorrentino, L.; Lavorgna, M.; Iannace, S. *Eur Polym J* 2011, 47, 925.
- Junker, M.; Alig, I.; Frisch, H. L.; Fleischer, G.; Schulz, M. *Macromolecules* 1997, 30, 2085.
- Madbouly, S. A.; Otaigbe, J. U.; Nanda, A. K.; Wicks, D. A. *Macromolecules* 2007, 40, 4982.
- Maji, P. K.; Bhowmick, A. K. *J Polym Sci Part A: Polym Chem* 2009, 47, 731.
- Wu, J.; Ge, Q.; Mather, P. T. *Macromolecules* 2010, 43, 7637.
- Romiszowski, P.; Sikorski, A. *J Mol Model* 2005, 11, 335.
- Auhl, D.; Kaschta, J.; Münstedt, H.; Kaspar, H.; Hintzer, K. *Macromolecules* 2006, 39, 2316.
- Gabriel, C.; Münstedt, H. *Rheol Acta* 2002, 41, 232.
- Jackson, C.; Chen, Y.; Mays, J. W. *J Appl Polym Sci* 1996, 59, 179.
- Rathgeber, S.; Gast, A. P.; Hedrick, J. L. *Appl Phys A* 2002, 74, 5396.
- Kulkarni, A. S. PhD thesis, University of Cincinnati, Ohio, 2007; p 189.
- Schweizer, K. S.; Fuchs, M.; Szamel, G.; Guenza, M.; Tang, H. *Macromol Theory Sim* 1997, 6, 1037.
- Gupta, T.; Adhikari, B. *Thermochim Acta* 2003, 402, 169.
- Chattopadhyay, D. K.; Webster, D. C. *Prog Polym Sci* 2009, 34, 1068.
- Berta, M.; Lindsay, C.; Pans, G.; Camino, G. *Polym Degrad Stab* 2006, 91, 1179.
- Vukovic, J.; Steinmeier, D.; Lechner, M.; Jovanovic, S.; Božić, B. *Polym Degrad Stab* 2006, 91, 1903.
- Hult, A.; Johansson, M.; Malmström, E. *Adv Polym Sci* 1999, 143, 1.
- Drobny, J. G. *Handbook of Thermoplastic Elastomers*; William Andrew Publishing/Plastics Design Library, 2007; Chapter 9, p 215.
- Liu, Y. R.; Huang, Y. D.; Liu, L. *Polym Degrad Stab* 2006, 91, 2731.
- Romo-Urbe, A.; Mather, P. T.; Haddad, T. S.; Lichtenhan, J. D. *J Polym Sci Part B: Polym Phys* 1998, 36, 1857.

43. Zuideveld, M.; Gottschalk, C.; Kropfinger, H.; Thomann, R.; Rusu, M.; Frey, H. *Polymer* 2006, 47, 3740.
44. Massa, D. J.; Shriner, K. A.; Turner, S. R.; Voit, B. I. *Macromolecules* 1995, 28, 3214.
45. Perstop Products. 2011 [Last accessed May 19, 2011]; Available from: <http://www.perstop.com/Products%20and%20Services/product-list.aspx>.
46. Xu, S.; Luo, R.; Wu, L.; Xu, K.; Chen, G. Q. *J Appl Polym Sci* 2006, 102, 3782.
47. Carr, P. L.; Davies, G. R.; Feast, W. J.; Stainton, N. M.; Ward, I. M. *Polymer* 1996, 37, 2395.
48. Emran, S. K.; Liu, Y.; Newkome, G. R.; Harmon, J. P. *J Polym Sci Part B: Polym Phys* 2001, 39, 1381.
49. Li, G.; Wang, L.; Ni, H.; Pittman, C. U., Jr. *J Inorg Organometall Polym* 2001, 11, 123.
50. Schwab, J. J.; Lichtenhan, J. D. *Appl Organom Chem* 1998, 12, 707.
51. Tan, J.; Jia, Z.; Sheng, D.; Wen, X.; Yang, Y. *Polym Eng Sci* 2011, 51, 795.
52. Wang, W.; Guo, Y. L.; Otaigbe, J. U. *Polymer* 2009, 50, 5749.
53. Raftopoulos, K. N.; Pandis, C.; Apekis, L.; Pissis, P.; Janowski, B.; Pielichowski, K.; Jaczewska, J. *Polymer* 2010, 51, 709.